Thermotropic Liquid Crystalline Complexes of Hydrogen-Bonded Poly(pyridylpyridinium dodecyl methacrylate) Bromide and Octylphenol

C. Geraldine Bazuin*,†,‡ and Christophe Brodin†

Centre de recherche en sciences et ingénierie des macromolécules (CERSIM), Département de chimie, Université Laval, Cité universitaire, Québec (QC), Canada G1K 7P4, and Département de chimie, Université de Montréal, C.P. 6128 Succursale Centre-Ville, Montréal (QC), Canada H3C 3J7

Received May 20, 2004; Revised Manuscript Received September 22, 2004

ABSTRACT: An ion-containing polyamphiphile, poly(ω-pyridylpyridinium dodecyl methacrylate) bromide, was successfully complexed with 4-octylphenol by hydrogen bonding, with no interference from the ionic moieties. Hydrogen bonding of the surfactant to the polymer is virtually complete up to near-equimolar phenol/pyridyl ratios. The complexation generates a well-behaved thermotropic liquid crystalline system from a low-melting surfactant and a polymer with ill-defined mesomorphism. The complex melts at relatively high temperatures into a liquid crystalline (smectic A) phase before becoming isotropic. The long period of the mesophase is almost identical to that of the polyamphiphile alone, is between the calculated lengths of the uncomplexed and complexed polymer repeat units, and is essentially independent of the complex stoichiometry. This can be rationalized by the same model presented in a previous publication for an ionically complexed polyamphiphile−surfactant system.

Introduction

The use of supramolecular chemistry, based on specific noncovalent interactions between dissimilar species, has allowed the development of a new class of liquid crystalline polymers (LCP's).[1−5] The interactions may involve hydrogen bonding, charge transfer, ionic interactions, or coordination complexation. Kato and Fréchet and co-workers were particularly active in developing a large variety of supramolecular side-chain LCP's, generally utilizing polymers with side chains terminated by benzoic acid and pyridine-containing small molecules such as stilbazole or bipyridine.[1] Hydrogen bonding between the pyridyl and acid functions induces an extended mesogen, which generates or stabilizes one or more mesophases. Many other groups have complexed various polymers, often polyelectrolytes, with complementary or oppositely charged simple surfactants.[6−8] Ruokolainen et al., for example, demonstrated that smectic-like organization takes place when poly(4-vinylpyridine) is complexed by hydrogen bonding with alkylphenols such as 3-pentadecylphenol.[9]

We also have been investigating side-chain LCP complexes, where the noncovalent interactions are located either close to or far from the polymer backbone. The former are based on simple functionalized polymers and small mesogenic molecules bearing complementary functions. For example, complexation between poly(acrylic acid) and an amine-functionalized mesogen via proton transfer generates a disordered mesophase that is inexistent in either component.[10] Other liquid crystalline complexes with stable smectic A phases over a wide temperature range were created using components with oppositely charged ionic functions.[11,12]

Recently, we synthesized a series of mesomorphic polyamphiphiles with long side chains terminated by different pyridinium groups.[13] Some of them were successfully complexed (far from the polymer backbone) with sulfonate surfactants via ion-exchange procedures.[14,15] In several cases, thermotropic liquid crystalline systems were obtained. One of the polyamphiphiles synthesized, shown in Figure 1, contains the pyridylpyridinium function. This provides an opportunity to explore the possibility of obtaining liquid crystalline polymer systems based on hydrogen-bond complexation with appropriately functionalized small molecules. To this end, we have chosen 4-octylphenol as the small molecule component. The polyamphiphile and the small molecule will be referred to henceforth as P12PP and C8ØOH, respectively.

These systems resemble those of Kato and co-workers,[1] where complexation takes place through hydrogen bonding far from the polymer backbone. The main differences lie in the inversion of the donor and acceptor groups in the polymer and small molecule and, most importantly, in the presence of the ionic moieties. The latter may potentially interfere with the desired hydrogen-bonding interactions, and thus this system also constitutes a test of the selectivity of the noncovalent interactions. Furthermore, the presence of ionic moieties can be useful for the additional control of the system's properties, such as the glass transition, which is generally raised by ionic interactions.[13,16] It should be mentioned that some small molecule systems involving both hydrogen-bonding and ionic interactions acting independently have been shown to be liquid crystalline;[4a,17−19] in particular, hydrogen-bonded complexes of an alkylpyridylpyridinium bromide with acid-functionalized[17] and, especially, hydroxyl-functionalized[18] molecules may be considered as small molecule analogues of the system described in this paper.

Experimental Section

Materials and Sample Preparation. The polyamphiphile, P12PP, was synthesized according to the procedure described previously.[14] Aqueous emulsion polymerization was effected with a monomer concentration of 0.1 mol L^{-1}, using 2 mol % sodium salt of 4,4′-azobis(4-cyanovaleric acid) (ACVA) as initiator and 4 mol % 1-dodecylmercaptan as chain transfer

† Université Laval.
‡ Current address: Université de Montréal.
* To whom correspondence should be addressed. E-mail: geraldine.bazuin@umontreal.ca.

10.1021/ma048994r CCC: $27.50
Published on Web 11/18/2004

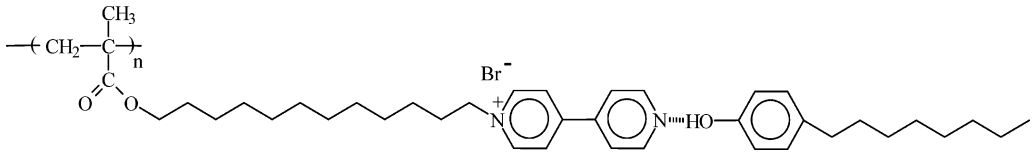

Figure 1. Molecular representation of the C8ØOH/P12PP complex.

agent (mol % relative to the monomer). This was followed by dialysis in frequently renewed ethanol/deionized water (starting at 50/50 v/v, progressively enriched to pure ethanol over a period of a week), using a Spectrapor membrane (VWR) with a molecular weight cutoff of 3500. The resulting polymer was estimated to have a molecular weight of about 10 000 according to osmometry measurements in ethanol.[20] 4-Octylphenol (99% purity) and 4-heptylpyridinium-4′-pyridine bromide (95% purity) were purchased from Aldrich and Acros, respectively, and used as received.

Complexes of various stoichiometries (0.25, 0.5, 0.75, 1.0, and 1.25 molar ratios of 4-octylphenol, C8ØOH, relative to the pyridylpyridinium repeat unit, along with a small amount of a 2.0 molar ratio sample) were prepared from ethanol solutions. Accurately weighed amounts of P12PP and C8ØOH were dissolved separately in ethanol (10 wt % concentration), giving completely transparent solutions. Then the C8ØOH solution was added all at once to the polymer solution, the combined solution remaining completely clear. This solution was heated to reflux under stirring for a week, after which the solvent was removed by slow evaporation at room temperature in a Petri dish. Finally, the product was dried under vacuum at 60 °C for 48 h (unless otherwise noted). The samples were stored at room temperature in a desiccator under vacuum until measurement (generally within 1 week).

Techniques. Infrared spectra were obtained from 100 scans at 2 cm^{-1} resolution, using a Nicolet Magna 560 spectrometer. Samples were prepared in the form of pressed KBr pellets. Temperature was controlled by a homemade oven and an Omega CDN7600 controller.

Thermogravimetric analysis was carried out under nitrogen flow at a heating rate of 10 °C/min using a Mettler TGA-50 balance. Differential scanning calorimetry (DSC) was performed using a Perkin-Elmer DSC-7, calibrated with indium and flushed with nitrogen, with 5−15 mg of sample crimped in standard aluminum pans. The complexes were melted at 150 °C for 5 min and then scanned between 0 and 150 °C at 20 °C/min (unless otherwise noted). C8ØOH was melted at 50 °C before scanning (at 10 °C/min). The glass transition temperatures are given by the midpoint of the heat capacity jump, and the other transition temperatures are given by the peak values (unless otherwise noted). No significant differences were observed in the transition temperatures and enthalpies of an equimolar complex that was scanned after 1, 2, and 4 days in a vacuum oven at 60 °C. Polarized optical microscopy (POM) measurements were made using a Zeiss Axioskop microscope equipped with a 25× Leica objective, a Mettler FP5 temperature controller, and a Mettler FP52 hot stage.

X-ray diffraction data were obtained with a Bruker diffractometer (Siemens Kristalloflex 760 generator), using a sealed tube anode providing Cu Kα radiation ($\lambda = 1.542$ Å) collimated by a graphite monochromator and a 0.8 mm pinhole. The diffraction pattern was recorded with a Bruker AXS two-dimensional wire-grid detector. Powdered samples were packed into 1.0 mm diameter Lindemann capillary tubes (Charles Supper Co.). Temperature was controlled by a modified Instec HCS400 heating stage and a STC200D Instec controller. All images were treated by subtracting a baseline image obtained using an empty capillary tube. The two-dimensional image was then integrated over 360° to plot the intensity as a function of 2θ. The d spacings were determined from the maximum of the diffraction peaks according to the Bragg equation, $n\lambda = 2d \sin \theta$, where n is an integer giving the order of the diffraction peak, θ is the angle of incidence, and λ is the wavelength of the X-ray beam used.

The calculated lengths (l_c) corresponding to a hypothetical single layer period were estimated using Hyperchem 5.0 software (Hypercube Inc.) for the lowest energy conformation of the side chain with the methylene units in an all-trans conformation. This molecular length, for the stoichiometric complex, corresponds to the distance from the outermost hydrogen (including van der Waals radius) of the methyl group on the P12PP backbone (the vinyl group being simulated by a *tert*-butyl moiety) to the furthest hydrogen (including van der Waals radius) of the terminal methyl group of C8ØOH. Following minimization, the hydrogen bond length is 2.5 Å, and the surfactant aromatic group lies at an angle relative to the polymer pyridine pyridinium group (which, in turn, is not in line with the all-trans alkyl chains).

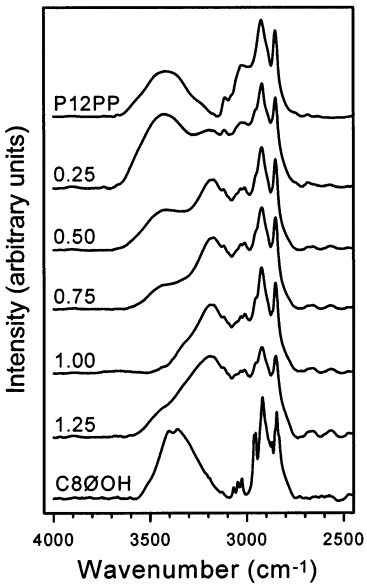

Figure 2. Infrared spectra in the 4000−2500 cm^{-1} region for the C8ØOH/P12PP complexes at the phenol/pyridine molar ratios indicated and for the two pure components separately.

Results

Infrared Analysis. Fourier transform infrared spectroscopy (FTIR) was used to confirm the anticipated hydrogen-bond interactions between the polyamphiphile and the phenol derivative. The most direct evidence for those interactions is found in the hydroxyl stretch region of the spectra between about 3100−3600 cm^{-1}, as shown in Figure 2 for the complexes of various stoichiometries and the two pure components at ambient temperature. Absorption maxima for C8ØOH are observed at about 3360 and 3400 cm^{-1}, with a very weak shoulder at about 3525 cm^{-1}. This can be compared with absorptions at 3525 and 3360 cm^{-1} observed in the spectrum of poly(4-vinylphenol) and attributed to free hydroxyls and a wide distribution of self-associated hydrogen-bonded hydroxyls, respectively.[21] For P12PP, a broad absorption band centered near 3420 cm^{-1} is observed, the intensity of which decreases significantly following more rigorous drying (10 days at 60 °C). Thus, it is attributed to strongly adsorbed water, possibly with a contribution from an overtone of the methacrylate C=O stretching mode.[22] Similarly, the absorption at 3400 cm^{-1} for C8ØOH, which was not subjected to drying prior to

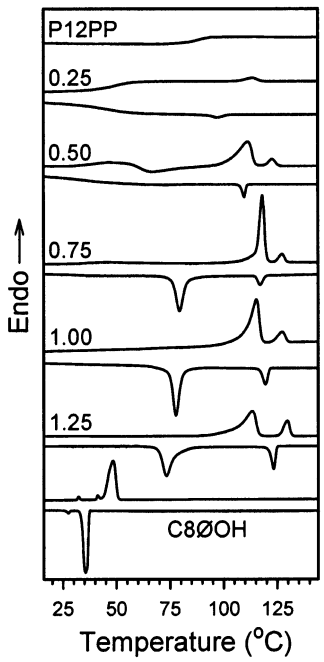

Figure 3. DSC heating and cooling thermograms (20 °C/min) for the C8ØOH/P12PP complexes at the molar ratios indicated as well as for P12PP and C8ØOH (heating only for the former; at 10 °C/min for the latter).

taking the spectrum, can be attributed to the presence of H_2O.

Focusing on the equimolar complex first, it is observed that the major absorption in this region is shifted to about 3180 cm^{-1}. Such a shift, indicative of "intermediate strength" hydrogen bonding,[23] is typically observed for phenol−pyridine hydrogen-bond interactions.[24] Only very weak absorptions remain near 3425 and 3350 cm^{-1}. This indicates that the phenol and pyridine groups are almost completely complexed by hydrogen bonding in the equimolar mixture. It may also be mentioned that there is no evidence of hydrogen bonding of phenol to the carbonyl group of the polymer; i.e., there is no indication of increased absorbance on the low wavenumber side of the C=O stretch at 1725 cm^{-1}, as was observed in blends of poly(methyl methacrylate) and poly(vinylphenol).[22]

The complexes of the other stoichiometries are similarly characterized by the band at 3180 cm^{-1}, most weakly for the 0.25 complex (Figure 2). The absorption peak near 3420 cm^{-1} decreases strongly with increasing C8ØOH content up to 1.0 molar ratio. This suggests that the surfactant displaces the adsorbed H_2O. In the spectrum of the 1.25 complex, the residual shoulders near 3425 and 3350 cm^{-1} are more intense than for the equimolar complex, consistent with the presence of excess surfactant in this complex. No major changes were observed in spectra of the equimolar sample taken at higher temperatures (up to nominally 130 °C) that were indicative of significant decomplexation. This does not rule out, of course, that the hydrogen bonds may be labile at higher temperatures.

Various spectral changes occur in the 1580−1625 cm^{-1} region as well; however, the presence of two phenyl bands for C8ØOH (1615 and 1600 cm^{-1}), which, unsurprisingly, also appear to be affected by hydrogen bonding, complicates the analysis of this region. The spectral changes in the C8ØOH/P12PP system are paralleled in the analogous nonpolymeric system composed of C8ØOH and 4-heptylpyridinium-4′-pyridine bromide (7PP). It is notable that the pyridine band is asymmetric in P12PP, suggesting the presence of an additional band on its lower wavenumber side, and two bands could be distinguished in 7PP;[20] this adds to the complexity of this region, which was thus not further analyzed.

Thermal Characteristics. The thermal stability of P12PP and the equimolar complex was verified first. Neither sample shows significant weight loss under a nitrogen atmosphere before about 150 °C, with 5% weight loss occurring at 210 and 220 °C, respectively. Degradation takes place in two main steps: the majority of the sample disappears between about 200 and 300 °C (65 and 75% of P12PP and the complex, respectively), with a second step in the region of 400 °C. Further analysis of the materials was limited to temperatures below 150 °C.

Figure 3 shows the DSC thermograms for the two pure components and the various complexes investigated. As described previously,[13] the only thermal event observed for the pure polyamphiphile is a glass transition, measured in the present case to be 87 °C (compared to 89 °C for a different batch of this polymer that was polymerized without transfer agent present[13]). 4-Octylphenol melts directly into the isotropic phase at an onset temperature of 44 °C and, on cooling, crystallizes at an onset of 37 °C; both transitions occur with high enthalpies (140 J/g), which is consistent with the nature of the transition.

In contrast, all of the complexes show two first-order transitions on heating, except for 0.25 which shows only one. These transitions occur at much higher temperatures than the melting point of C8ØOH, indicating that they are related to the complexes. The higher temperature transition is of low intensity and displays little supercooling, whereas the lower one is of higher intensity and displays significant supercooling. These characteristics suggest that the complexes are thermotropic liquid crystals, with an ordered phase at lower temperatures and a liquid crystalline mesophase at higher temperatures. This is supported by POM observations, showing a solid birefringent material at temperatures below the first transition, a fluid birefringent material between the two transitions, and an optically isotropic liquid above the second transition. It is also noteworthy that the 0.5 complex does not crystallize on cooling in the time scale of the DSC thermogram, but a broad recrystallization endotherm is observed near 65 °C on heating (also noted by POM).

The temperatures and enthalpies of the different transitions in the complexes are given in Table 1, and the transition temperature variations as a function of composition are shown in Figure 4. The higher transition temperature depends little on the complex composition for phenol/pyridine molar ratios between 0.75 and 2.0 and shows a mild decrease (more marked on cooling than on heating) with decreasing molar ratio from 0.75 to 0.25. The corresponding enthalpies undergo a small but continuous increase with molar ratio from 1 J/g for the 0.25 complex to almost 5 J/g for the 2.0 complex and the disappearance of this transition for the 0.25 complex (as confirmed by X-ray analysis; see below). The lower transition temperature and enthalpy show a shallow maximum in the 0.75 to 1.0 molar ratio range on heating, with a drastic reduction for the 2.0 complex. The significance of these tendencies will be discussed later.

Table 1. Transition Temperatures (T_g, T_1, T_2), Heat Capacity Increments (ΔC_p), and Enthalpies (ΔH_1, ΔH_2) for the Various C8ØOH/P12PP Complexes

			T_1 (°C)		ΔH_1 (J/g)		T_2 (°C)		ΔH_2 (J/g)	
molar ratio	T_g (°C)	ΔC_p (J/(g °C))	heat	cool	heat	cool	heat	cool	heat	cool
0.25	49	0.3					113	97	0.9	−0.8
0.5	37	0.3	111		12		123	110	1.5	−1.6
0.75	33	0.3	118	79	20	−14	127	117	2.2	−2.4
1.0			115	78	17	−14	127	119	2.7	−3.0
1.25			113	73	16	−13	130	123	3.5	−3.8
2.0[a]			∼85[b]	∼40[b]	∼5	∼−5	126	123	4.4	−4.6

[a] Scanned at 5 °C/min.[25] [b] Broad.

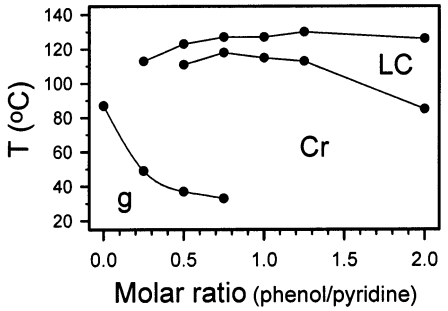

Figure 4. Transition temperatures (glass transition, melting point, and clearing point) as a function of composition for the C8ØOH/P12PP complexes, obtained from DSC heating thermograms (g: glassy; Cr: crystalline; LC: liquid crystalline).

Finally, a glass transition is detectable in the DSC thermograms for molar ratios of 0.75 and below. Its value decreases with increase in C8ØOH content, reflecting a plasticization effect of the complexed surfactant, which effectively increases the length of the side chains. This effect is attenuated as crystallization sets in. The heat capacity increments at the T_g are constant near 0.3 J/(g °C).

Structural Analysis. X-ray diffractograms of the complexes below the lower temperature DSC transition, between the two DSC transitions, and above the higher temperature DSC transition are given in Figure 5. For comparison, diffractograms of P12PP and C8ØOH are shown in Figure 6. The latter shows clearly the crystalline nature of C8ØOH at low temperature, with a long period (29.4 Å) corresponding to nearly twice the extended molecular length of C8ØOH (estimated as 17 Å). Above the melting point, where C8ØOH is isotropic between crossed polarizers, local order persists as evidenced by the halos at wide and intermediate angles, corresponding to average periods of 4.7 and 19.7 Å, respectively (the latter period being close to a single extended molecular length of C8ØOH). P12PP, as shown before,[13] is weakly birefringent between crossed polarizers and possesses a disordered smectic A-like morphology of short correlation lengths, with a long period (34−35 Å) that lies between one and two extended molecular lengths of the repeat unit (29 Å).

In the ambient temperature phase of the complexes of higher molar ratios (≥0.75), the wide-angle region is characterized by a series of weak diffraction peaks superposed on a broad halo, indicating, in accordance with the DSC data, partial crystallinity in the sample. The pattern of the peaks is distinct from that for C8ØOH alone, indicating that they are not due to phase-separated surfactant. The crystallinity in the 1.25 sample appears less well-defined than in the two lower molar ratio samples, possibly due to the presence of excess (melted) C8ØOH. In the temperature region of the high-enthalpy DSC transition, the wide-angle peaks disappear, thus clearly identifying this transition with the melting point of the crystalline phase. In the intermediate and highest temperature phases, as well as at ambient temperature for the lowest molar ratio complexes, there is only a broad halo at wide angles, indicative of the lack of short-range order.

At small angles, both the crystalline and intermediate phases are characterized by an intense first-order diffraction peak and a second much weaker diffraction peak, whose reciprocal spacings are in a 1:2 ratio. This is consistent with lamellar ordering for both phases and, along with the wide-angle halo, allows the intermediate phase to be identified as a smectic A or C phase. The two small-angle peaks remain present in the isotropic phase, but with much lower intensity and greater broadness. This indicates a tendency to organize into cybotactic-like structures (i.e., lamellar-like structures with very short correlation lengths).

The Bragg spacings calculated from the small-angle peaks of the complexes and pure components at selected temperatures are given in Table 2. First, it is noted that the ambient temperature values for the complexes are about 1−4 Å smaller after the heating cycle than before. This was also observed by Vuillaume et al.[13,14] and was attributed to loss of residual water after exposure to high temperature or to slow thermal equilibrium. Second, the Bragg spacings tend to decrease somewhat with increasing temperature and vice versa. As shown in Figure 7, where the Bragg spacings are plotted as a function of temperature for the equimolar complex, the lamellar thickness evolves discontinuously in the transition regions (observed clearly only for the 0.75 to 1.25 complexes). Third, the Bragg spacings show no systematic variation as a function of composition, being about 36 ± 1 and 34 ± 1 Å at ambient temperature before heating and after cooling, respectively. Furthermore, they are almost identical to that measured for the uncomplexed P12PP. Finally, the Bragg spacings are always significantly less than the end-to-end extended molecular length of the hydrogen-bonded polymer repeat unit and C8ØOH (which is about 43 Å as determined by Hyperchem or about 47 Å if the two constituents are manually aligned end-to-end in as linear a fashion as possible using CPK molecular models), but much greater than that of a single polymer repeat unit (29 Å).

Discussion

The complexation of 4-octylphenol to poly(ω-pyridylpyridinium dodecyl methacrylate) bromide evidently occurs selectively between the phenol and pyridyl functionalities, via hydrogen bonding, with no interference from the ionic pyridinium bromide moiety. This interaction allows a straightforward lengthening of the side chain, including an effective lengthening of the rigid segment, which is no doubt responsible for the well-

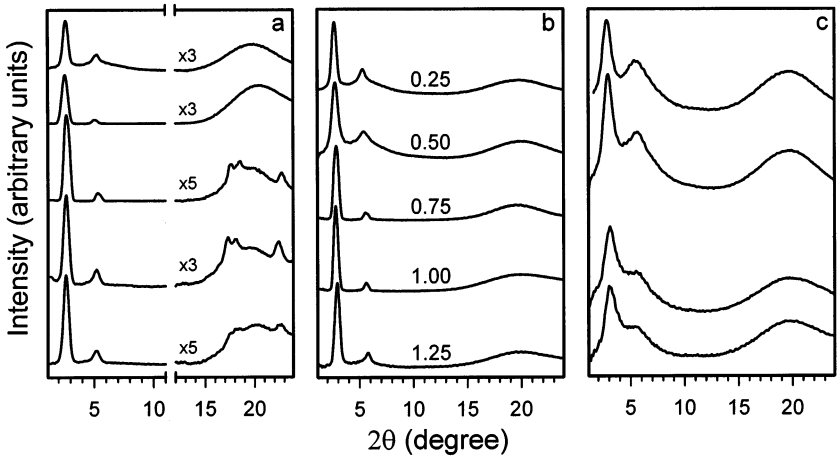

Figure 5. X-ray diffractograms of the complexes of various molar ratios [(from top to bottom as indicated in (b)]: (a) at 30 °C (after cooling from 130 °C), (b) in the mesophase (at about 100 °C), and (c) the isotropic phase (130 °C; not available for 0.75). In (a), the right-hand halves of the curves were multiplied by the factor indicated relative to the left-hand halves. The temperatures quoted are nominal.

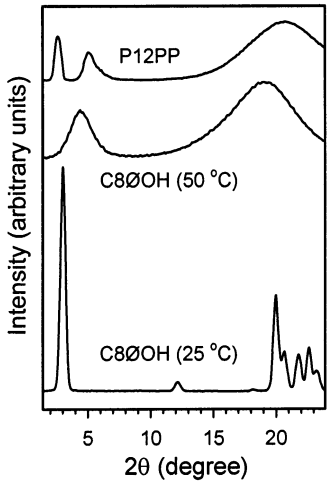

Figure 6. X-ray diffractograms of P12PP at ambient temperature and of C8ØOH at the temperatures indicated.

behaved thermotropic characteristics of the complexed system. In this respect, the present system resembles those developed by Kato and Fréchet,[1] as mentioned in the Introduction, and contrasts with the ionically bonded polyamphiphile−surfactant complexes investigated by Vuillaume and Bazuin,[14] where the location of the pyridinium moiety on the inner side of the rigid segment (i.e., on the polymer spacer side) necessitates some kind of lateral overlap of at least part of the polymer side chain and surfactant.

The complexation generates a crystalline phase that is much more stable than that of C8ØOH as well as being structurally distinct from the latter. The crystallinity most likely involves only the tail ends of the complexed surfactant, as also observed frequently for long aliphatic side-chain polymers[26] and for other polymer−surfactant complexes including the above-mentioned ionically complexed polyamphiphile−surfactant system.[14] In the presence of a significant excess of C8ØOH (2.0 molar ratio), the crystallization temperature is drastically reduced, which can be attributed to interference by the excess melted surfactant in the crystallization process (the melting point is much less affected). Reducing the complexation below equimolar must lead to increasingly smaller and imperfect crystals, as observed for any crystallizing side-chain copolymers,

Table 2. X-ray Scattering Data Obtained for C8ØOH, P12PP, and the C8ØOH/P12PP Complexes of the Molar Ratios Indicated at Selected Temperatures (d_1, d_2: d Spacings for the First and Second Small-Angle Peaks, Respectively; RT: Ambient Temperature)

sample (molar ratio)	temp (°C)	d_1 (Å)	$2d_2$ (Å)
P12PP[a]	RT[b]	34.5	34.6
C8ØOH	RT[b]	29.4	
	50	19.7[c]	
0.25	RT[b]	38.1	38.0
	80	33.9	33.0
	110	33.1	33.4
	130	31.2	32.1
	RT[d]	33.7	34.0
0.50	RT[b]	35.6	35.9
	90	34.8	35.1
	110	31.8	32.4
	130	30.1	31.1
	RT[d]	34.5	34.9
0.75	RT[b]	36.7	36.3
	70	36.9	36.5
	90	35.6	35.4
	110	33.2	33.1
	130	29.2	31.2
	RT[d]	32.7	32.9
1.0	RT[b]	36.0	35.8
	70	36.4	36.1
	100	32.5	33.1
	130	28.4	
	RT[d]	33.5	33.9
1.25	RT[b]	34.4	34.8
	80	34.2	34.9
	110	31.8	32.0
	130	28.3	
	RT[d]	33.5	33.9

[a] Dried for 3 days at 60 °C prior to the measurement. [b] Before heating. [c] From the maximum of the halo. [d] After cooling.

such that, in the time scale of the DSC experiment, crystallization is suppressed on cooling when only half of the side chains are complexed and is completely inhibited when only a quarter of the side chains are complexed.

The liquid crystalline phase that is generated at higher temperatures appears to be lamellar and, without evidence for preferential tilting of the molecular axis relative to the layer normal, can be concluded to be a smectic A mesophase. The slight decrease in the lamellar thickness with increasing temperature observed in the mesophase (Figure 7) is consistent with this assignment.[27] It was also noted that the long spacing obtained

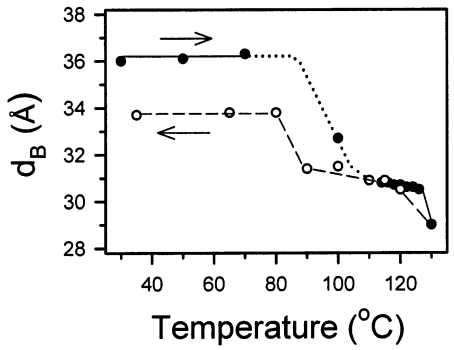

Figure 7. Lamellar thickness (d_B) as a function of temperature for the equimolar C8ØOH/P12PP complex on heating (filled circles) and cooling (open circles); the lines are a guide to the eye, with the dotted segment representing an estimated evolution of d_B in the transition region during heating.

from the X-ray data is very similar in the crystalline and liquid crystalline phases and essentially the same as that of the uncomplexed polyamphiphile. This was also observed for the ionically bonded polyamphiphile−surfactant complexes previously investigated, including for surfactants of very different lengths.[14,28] For the latter, one possible model that was evoked to rationalize this observation involves the complexed surfactant folding back along the polymer side chain such that the surfactant alkyl chain is mixed with the alkyl spacer of the polymer.[14] An argument against this packing arrangement was the difficulty of rationalizing the tail-end crystallinity observed for the longest surfactant. In the present system, not only is this latter objection still valid but also the location of the H-bond at the terminal end of the polymer side chain, along with the directionality of the H-bond, renders this model practically inconceivable. On the other hand, the data from the present system can be rationalized by the second model proposed: in this model, lamellar subdomains, composed of the polymer side chain extended by the complexed surfactant, randomly alternate along the lamellar plane in the up−down direction while preserving lateral continuity of the ionic subplanes. This results in the overall repeat distance being determined primarily by the polyamphiphile due to the connectivity between the pyridinium moieties and the polymer backbone, a situation to which the complexed surfactant can adjust given the flexibility of the alkyl chains (see ref 14 for details).

Finally, it may be remarked that the pyridyl−phenol hydrogen bonds may well become dynamic in the liquid crystalline mesophase. This lability may contribute to the significant mobility observed in this phase.

Conclusions

This study has shown that the pyridyl terminal moiety in the side-chain polyamphiphile, poly(ω-pyridylpyridinium dodecyl methacrylate) bromide, can be successfully complexed with alkyl phenol surfactants via hydrogen bonding up to equimolar proportion, with no apparent interference from the nearby pyridinium bromide ion pair. This complexation generates, from a low-melting surfactant and a polymer with poorly defined mesomorphism, a well-behaved thermotropic liquid crystalline material with a relatively high-melting crystalline phase and a liquid crystalline mesophase that is most likely smectic A in nature. The long period of both phases is similar to that of the uncomplexed polyamphiphile, as observed also in other polyamphiphile−surfactant complexes investigated, and can be rationalized by the same model as proposed in ref 14, where the overall lamellar spacing is determined primarily by the parent polyamphiphile and which involves random flipping of subdomains located laterally along the lamellar planes.

Acknowledgment. The financial support of NSERC (Canada) and FCAR (Québec) is gratefully acknowledged. We also thank Pascal Vuillaume for his help in synthesizing the polymer, Qian Zhang for his aid in finalizing the figures, and Qing Lu for verifying the Hyperchem models.

References and Notes

(1) Kato, T. *Struct. Bonding (Berlin)* **2000**, *96*, 95 and references therein. Kato, T. In *Handbook of Liquid Crystals*; Demus, D., Goodby, J. W., Gray, G. W., Spiess, H. W., Vill, V., Eds.; Wiley-VCH: Weinheim, 1998; Vol. 2B, p 969 and references therein.
(2) Lehn, J.-M. *Supramolecular Chemistry—Concepts and Perspectives*; VCH: Weinheim, 1995. Krische, M. J.; Lehn, J.-M. *Struct. Bonding (Berlin)* **2000**, *96*, 3.
(3) Bazuin, C. G. In *Mechanical and Thermophysical Properties of Polymer Liquid Crystals*; Brostow, W., Ed.; Chapman and Hall: London, 1998; Vol. 3, Chapter 3 and references therein.
(4) (a) Paleos, C. M.; Tsiourvas, D. *Liq. Cryst.* **2001**, *28*, 1127 and references therein. (b) Paleos, C. M.; Tsiourvas, D. *Angew. Chem., Int. Ed. Engl.* **1995**, *34*, 1696 and references therein.
(5) Lee, C. M.; Griffin, A. C. *Macromol. Symp.* **1997**, *117*, 281 and references therein.
(6) Antonietti, M.; Thünemann, A. *Curr. Opin. Colloid Interface Sci.* **1996**, *1*, 667 and references therein.
(7) MacKnight, W. J.; Ponomarenko, E. A.; Tirrell, D. A. *Acc. Chem. Res.* **1998**, *31*, 781 and references therein.
(8) Zhou, S.; Chu, B. *Adv. Mater.* **2000**, *12*, 545 and references therein.
(9) Ruokolainen, J.; ten Brinke, G.; Ikkala, O.; Torkkeli, M.; Serimaa, R. *Macromolecules* **1996**, *29*, 3409.
(10) Tork, A.; Bazuin, C. G. *Macromolecules* **2001**, *34*, 7699. Bazuin, C. G.; Boivin, J.; Tork, A.; Tremblay, H.; Bravo-Grimaldo, E. *Macromolecules* **2002**, *35*, 6893.
(11) Bazuin, C. G.; Tork, A. *Macromolecules* **1995**, *28*, 8877.
(12) Tibirna, C. M. Ph.D. Thesis, Dép. de chimie, Université Laval, Québec, 2003.
(13) Vuillaume, P. Y.; Galin, J.-C.; Bazuin, C. G. *Macromolecules* **2000**, *33*, 781.
(14) Vuillaume, P. Y.; Bazuin, C. G. *Macromolecules* **2003**, *36*, 6378.
(15) Vuillaume, P. Y.; Bazuin, C. G. *Am. Chem. Soc. Polym. Prepr.* **1999**, *40* (2), 490; full publication in preparation.
(16) Eisenberg, A.; Kim, J. S. *Introduction to Ionomers*; John Wiley & Sons: New York, 1998.
(17) Bernhardt, H.; Weissflog, W.; Kresse, H. *Liq. Cryst.* **1998**, *24*, 895. Sahin, Y. M.; Diele, S.; Kresse, H. *Liq. Cryst.* **1998**, *25*, 175.
(18) Kresse, H. *Liq. Cryst.* **1998**, *25*, 437.
(19) Tsiourvas, D.; Paleos, C. M.; Skoulios, A. *Liq. Cryst.* **1999**, *26*, 953.
(20) Brodin, C. Ph.D. Thesis, Dép. de chimie, Université Laval, Québec, 2003.
(21) Coleman, M. M.; Moskala, E. J.; Painter, P. C.; Walsh, D. J.; Rostami, S. *Polymer* **1983**, *24*, 1410.
(22) Dong, J.; Ozaki, Y. *Macromolecules* **1997**, *30*, 286.
(23) Coleman, M. M.; Graf, J. F.; Painter, P. C. *Specific Interactions and the Miscibility of Polymer Blends*; Technomic Publishing Co.: Lancaster, 1991.
(24) Isasi, J. R.; Cesteros, L. C.; Katime, I. *Macromolecules* **1994**, *27*, 2200.
(25) For comparison, it was noted that an equimolar sample scanned at 5 °C/min resulted in a melting point (T_1 on heating) and clearing point (T_2 on heating) that was 2 °C lower than when scanned at 20 °C/min, whereas on cooling, T_2 and T_1 were 3 and 7 °C higher, respectively.
(26) Platé, N. A.; Shibaev, V. P. *J. Polym. Sci., Macromol. Rev.* **1974**, *8*, 117.

(27) A two-dimensional diffractogram of an oriented ionically bonded complex, which is analogous to the present one and which has an almost identical lamellar spacing, certainly indicated a smectic A mesophase (see ref 14).

(28) Vuillaume, P. Y. Ph.D. Thesis, Dép. de chimie, Université Laval, Québec, 2000.

MA048994R